Journal of Hazardous Materials 183 (2010) 182–188

Contents lists available at ScienceDirect

Journal of Hazardous Materials

journal homepage: www.elsevier.com/locate/jhazmat

Zinc oxide particles induce inflammatory responses in vascular endothelial cells via NF-κB signaling

Tsui-Chun Tsou[a,*], Szu-Ching Yeh[a], Feng-Yuan Tsai[a], Ho-Jane Lin[a], Tsun-Jen Cheng[b], How-Ran Chao[c], Lin-Ai Tai[d]

[a] Division of Environmental Health and Occupational Medicine, National Health Research Institutes, Zhunan, Miaoli County, Taiwan
[b] Institute of Occupational Medicine and Industrial Hygiene, National Taiwan University, Taipei, Taiwan
[c] Department of Environmental Science and Engineering, National Pingtung University of Science and Technology, Neipu, Pingtung, Taiwan
[d] Center for Nanomedicine Research, National Health Research Institutes, Zhunan, Miaoli County, Taiwan

ARTICLE INFO

Article history:
Received 3 February 2010
Received in revised form 3 June 2010
Accepted 3 July 2010
Available online 31 July 2010

Keywords:
Zinc oxide
Endothelium
Inflammation
NF-κB
Adhesion molecules
Cytokines

ABSTRACT

This study investigated inflammatory effects of zinc oxide (ZnO) particles on vascular endothelial cells. The effects of 50 and 100-nm ZnO particles on human umbilical vein endothelial cells (HUVECs) were characterized by assaying cytotoxicity, cell proliferation, and glutathione levels. A marked drop in survival rate was observed when ZnO concentration was increased to 45 μg/ml. ZnO concentrations of ≤3 μg/ml resulted in increased cell proliferation, while those of ≤45 μg/ml caused dose-dependent increases in oxidized glutathione levels. Treatments with ZnO concentrations ≤45 μg/ml were performed to determine the expression of intercellular adhesion molecule-1 (ICAM-1) protein, an indicator of vascular endothelium inflammation, revealing that ZnO particles induced a dose-dependent increase in ICAM-1 expression and marked increases in NF-κB reporter activity. Overexpression of IκBα completely inhibited ZnO-induced ICAM-1 expression, suggesting NF-κB plays a pivotal role in regulation of ZnO-induced inflammation in HUVECs. Additionally, TNF-α, a typical inflammatory cytokine, induced ICAM-1 expression in an NF-κB-dependent manner, and ZnO synergistically enhanced TNF-α-induced ICAM-1 expression. Both 50 and 100-nm ZnO particles agglomerated to similar size distributions. This study reveals an important role for ZnO in modulating inflammatory responses of vascular endothelial cells via NF-κB signaling, which could have important implications for treatments of vascular disease.

1. Introduction

A recently published commentary focused on the safe handling of nanotechnology has recommended strategic research to support sustainable nanotechnologies by maximizing benefits and minimizing environmental and health risks [1]. Although recent epidemiologic studies have demonstrated a correlation between exposure to fine particulate matter in air pollution and an increased incidence of cardiovascular morbidity and mortality [2–4], the mechanisms behind this correlation remain largely unknown. Ultrafine particles (<100 nm) have been reported to be particularly pathologically relevant because of their small size and high reactivity. Of particular relevance to the present study, ultrafine particles have been shown to cross the pulmonary epithelial barrier into the bloodstream [5–7], directly exposing the vascular endothelium to particles.

ZnO nanoparticles (nano-ZnO) are a newly developed inorganic material with multiple applications. Minimization of the crystal nanoparticles results in changes in the surface electron structure as well as in the crystal surface area, which elicit many unique properties from the nanoparticles, especially those related to catalyses, optics, magnetics, and mechanics. Recently, nano-ZnO has been applied extensively in many different fields, including ceramics, chemical industry, electronic industry, biology, and medicine. It has also been demonstrated that nano-ZnO causes activation of inflammation in vascular endothelial cells [8]. Previous studies have revealed that endothelial dysfunction is a critical early step in atherogenesis [9,10]. Moreover, atherosclerosis is thought to be a chronic inflammatory disease of the vessel wall [9]. Thus, inflammation and endothelial dysfunction have been shown to intimately link to the pathogenesis of cardiovascular disease [10]. Of these, the links between nano-ZnO exposure, inflammation, endothelial dysfunction, and cardiovascular disease might be of particular importance. During this process, inflammation and oxidative stress (or redox status) seem to play key roles in the development of cardiovascular diseases such as atherosclerosis.

* Corresponding author. Tel.: +886 37 246 166x36511; fax: +886 37 587 406.
E-mail address: tctsou@nhri.org.tw (T.-C. Tsou).

0304-3894/$ – see front matter © 2010 Elsevier B.V. All rights reserved.
doi:10.1016/j.jhazmat.2010.07.010

Table 1
ZnO particles used in this study.[a]

Material	Particle size (nm)	Surface area (m^2/g)	Purity (%)	Vender/cat.#
50 nm ZnO	<50 (BET[b])	>10.8	>97.0	Aldrich/677450
100 nm ZnO	<100	15–25	≥98.5	Aldrich/544906

[a] Data were taken from the manufacturer's data sheets.
[b] Particle size was measured by the Brunauer–Emmett–Teller method.

Previous studies have revealed a growing appreciation of cytokines as central players in the pathogenesis of atherosclerosis. Various pathophysiological phenomena may stimulate cytokine release, including modified LDL [11,12], free radicals [13], hemodynamic stress [14,15], and hypertension [16]. Cytokines differentially affect atherogenesis, with distinct cytokines directing pro- as well as anti-atherogenic processes, modulating plaque characteristics and clinical outcomes [17]. Cytokines influence the development of atherosclerosis with the formation of complex atherosclerotic plaques, which may in turn lead to acute thromboembolic complications such as myocardial infarction or stroke [17]. Recent studies have highlighted a central role for the vascular endothelium in modulating the inflammatory response [18].

The present study aimed to determine the underlying mechanism by which nano-ZnO caused the activation of inflammatory responses in vascular endothelial cells. Although our results failed to differentiate the biological effects induced by 50 and 100-nm ZnO particles due to the unavoidable agglomeration of these particles in the culture medium, this study reveals an important role for ZnO in modulating the inflammatory responses of vascular endothelial cells via NF-κB signaling. The synergistic effect of ZnO on inflammatory cytokine-induced vascular endothelium dysfunction could be critical in the development of cardiovascular disease.

2. Materials and methods

2.1. Materials

ZnO particles (50 and 100 nm) were purchased from Sigma–Aldrich, Inc. (St. Louis, MO, USA). MTT (3-[4,5-dimethylthiazol-2-yl]-2,5-diphenyltetrazolium bromide) was obtained from Calbiochem (San Diego, CA, USA). Rabbit polyclonal antibodies against ICAM-1 (sc-7891) and IκBα (sc-847) and a goat polyclonal antibody against p-IκBα (sc-7977) were purchased from Santa Cruz Biotechnology (Santa Cruz, CA, USA). A mouse monoclonal antibody against actin (MAB1501) was purchased from Chemicon Int. Inc. (Temecula, CA, USA). TNF-α (11371843001) was obtained from Roche Applied Science (Mannheim, Germany). *Pfu* DNA polymerase (M774A) was obtained from Promega Corp. (Madison, WI, USA). Dulbecco's phosphate-buffered saline (DPBS) was obtained from Gibco (Grand Island, NY, USA). M199 medium was obtained from Life Technologies (Grand Island, NY, USA). Fetal bovine serum (FBS) was obtained from HyClone (Logan, UT, USA). Penicillin (10,000 units/ml)/streptomycin (10,000 μg/ml) solution was obtained from Invitrogen Corp. (Carlsbad, CA, USA). Gentamycin sulfate was purchased from Biological Industries (Kibbutz Beit Haemek, Israel).

2.2. Preparation of ZnO particles

Table 1 lists the physical characteristics of the two types of ZnO particles used in this study. Stock suspensions (30 mg/ml) of each type of ZnO particle (50 nm or 100 nm) were prepared in sterile, ultrapure Milli-Q water. Each suspension was probe sonicated for 30 s prior to exposure and characterization. For the *in vitro* studies, a stock solution was diluted serially to yield final concentrations ranging from 0.1 to 75 μg/ml in the culture medium (M199).

2.3. Isolation and treatments of HUVECs

HUVECs were obtained by collagenase digestion of umbilical veins, as described previously [19] with modifications [20]. The isolated HUVECs were seeded into culture dishes coated with 0.1% gelatin and grown in M199 medium containing 20% fetal bovine serum (FBS), 2 mM L-glutamine, endothelial cell growth supplement (30 μg/ml) (Sigma–Aldrich, St. Louis, MO), penicillin (100 U/ml), streptomycin (100 μg/ml), and gentamycin (100 μg/ml). Unless indicated, HUVECs were seeded into 6-well dishes at a density of 2×10^5 cells/well. For experiments using adenovirus infection, HUVECs were infected with one or two recombinant adenoviruses at a multiplicity of infection of 50 plaque-forming units (pfu)/cell for 24 h.

2.4. MTT assay

For cytotoxicity and cell proliferation assays, HUVECs were seeded into 6-well dishes at densities of 2×10^5 and 2×10^4 cells/dish, respectively. After ZnO treatments, survival and proliferation rates were evaluated using an MTT assay. After treatments, 200 μl of MTT (5 mg/ml) was added into the culture medium, and then, the cells were cultured for another 4 h. The assay was performed as previously described [21] with minor modifications [22]. The assay is based on the cleavage of MTT, a yellow tetrazolium salt, to purple formazan crystals by the succinate-tetrazolium reductase system, belonging to the respiratory chain of mitochondria. The formazan crystals formed were dissolved in 1 ml of solution containing 10% SDS and 0.01 M HCl. The resulting colored solution was quantified using an Anthos BT3 ELISA reader (Anthos Labtec Instruments, Wals, Austria) at $OD_{595\,nm}$. In each set of experiment, data were expressed as relative survival rates or relative proliferation rates as normalized to the untreated control. The untreated control was set as 100%.

2.5. Measurement of intracellular glutathione concentration

Following treatments, intracellular glutathione levels were measured using a Bioxytech GSH/GSSG-412 assay kit (Oxis International Inc., Portland, OR, USA), as described previously [22]. In our assay system, we measured the overall ratio of GSH/GSSG > 100/1, indicating that most glutathione molecules in HUVECs existed in reduced form. These data are comparable to our previous results as well as those of other studies [22,23]. Since most of the glutathione in these cell lines existed in reduced form, the intracellular GSH concentration was used to represent the intracellular glutathione concentration in this study.

2.6. Immunoblot analysis

Following treatments, cells were lysed in ice-cold RIPA buffer (50 mM Tris–HCl, pH 7.5, 5 mM EDTA, 1 mM EGTA, 1% Triton X-100, 0.25% sodium deoxycholate) containing PMSF (2 mM), aprotinin (2 μg/ml), leupeptin (2 μg/ml), NaF (2 mM), Na_3VO_4 (2 mM), and β-glycerophosphate (0.2 mM). The cell lysates were subjected to SDS-PAGE and immunoblot analysis, as described previously [22]. The blots were probed with primary antibodies against ICAM-1,

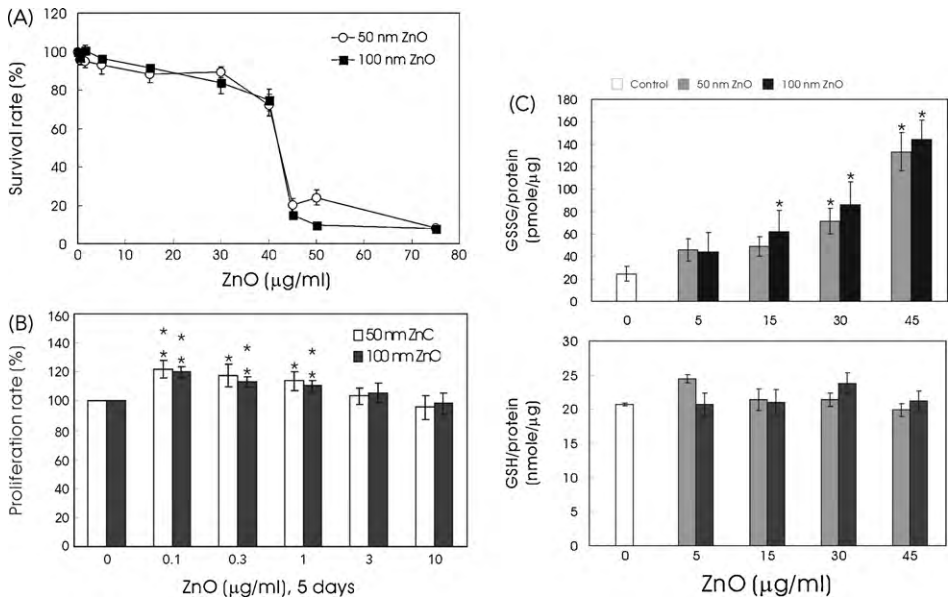

Fig. 1. Characterization of the effects of ZnO on cytotoxicity, proliferation, and glutathione levels in HUVECs. (A) For the cytotoxicity assay, HUVECs were left untreated or treated with 0.5, 1.5, 5, 15, 30, 40, 45, 50 or 75 μg/ml of ZnO (50 nm or 100 nm) for 24 h. Following treatments, survival rates were determined. The data are presented as means ± SE ($n = 6$) and are expressed as relative survival rates compared to that of the untreated control. (B) For the proliferation assay, HUVECs were left untreated or treated with 0.1, 0.3, 1, 3 or 10 μg/ml of ZnO (50 nm or 100 nm) for 5 days. Following treatments, relative proliferation rates were determined. The data are presented as means ± SE ($n = 6$) and are expressed as relative proliferation rates compared to that of the untreated control. $^{*}p < 0.05$, $^{**}p < 0.01$ versus the untreated control. (C) To determine intracellular glutathione levels, the cells were left untreated or treated with 5, 15, 30 or 45 μg/ml of ZnO (50 nm or 100 nm) for 24 h. Following treatments, intracellular levels of GSSG (top) and GSH (bottom) were analyzed. The data are presented as means ± SE ($n = 3$) and are expressed as GSSG/protein (pmol/μg) and GSH/protein (nmol/μg). $^{*}p < 0.05$ versus the untreated control.

p-IκBα, IκBα or actin. HRP-conjugated secondary antibodies and Western Lightning Chemiluminescence Reagent Plus (PerkinElmer Life Sciences, Boston, MA, USA) were used to reveal specific protein bands. Protein band intensities were quantified by densitometry.

2.7. Construction of recombinant adenoviruses

The IκBα Dominant-Negative Vector Set (631923) (Clontech Laboratories, Inc., Mountain View, CA, USA) contained two vectors, pCMV-IκBα and pCMV-IκBαM, for studying NFκB and related signaling pathways. pCMV-IκBα expresses wild-type IκBα protein. pCMV-IκBαM contains a mutated form of IκBα with serine-to-alanine mutations at residues 32 and 36. This mutated form does not undergo signal-induced phosphorylation and thus remains bound to NFκB. Both genes are expressed from the constitutive CMV promoter.

The IκBα gene in pCMV-IκBα and pCMV-IκBαM was amplified by PCR using *pfu* DNA polymerase. Amplified DNA fragments were digested by *KpnI* and *SalI*. After separation by agarose gel electrophoresis, the purified *KpnI*/*SalI*-digested IκBα fragments were cloned into *KpnI*/*SalI*-digested pAdTrack-CMV. In addition to the cloned DNA fragments, pAdTrack-CMV carries a built-in CMV-driven green fluorescent protein (GFP) tracer. The recombinant adenoviruses were generated using the AdEasy™ Adenoviral Vector System (Stratagene, La Jolla, CA, USA). Three recombinant adenoviruses, AdV-GFP (expressing a built-in GFP tracer), AdV-IκBα-wt (expressing a wild-type IκBα under the CMV promoter with a built-in GFP tracer), and AdV-IκBα-m (expressing a mutated IκBα under the CMV promoter with a built-in GFP tracer), were generated and amplified according to the manufacturer's instructions.

A 2380-bp DNA fragment containing five copies of the NFκB response element, a TATA box, and a firefly luciferase gene in pNFκB-Luc (Stratagene, La Jolla, CA, USA), was amplified by PCR using *pfu* DNA polymerase. The amplified DNA fragment was digested by *KpnI* and *SalI*. After separation by agarose gel electrophoresis, the purified *KpnI*/*SalI*-digested DNA fragment was cloned into the *KpnI*/*SalI*-digested pACCMV.pLpA vector [24]. The function of the CMV promoter of the pACCMV.pLpA vector used here had been abolished. The recombinant adenovirus AdV-NFκB-Luc was generated by homologous recombination between the pJM17 plasmid [25] and the pACCMV.pLpA vector in 293 human embryo kidney cells.

2.8. Measurements of NFκB reporter activity

HUVECs were seeded into 6-well dishes at a density of 2×10^5 cells/well. HUVECs were infected with the recombinant adenovirus AdV-NFκB-Luc at a multiplicity of infection of 50 pfu/cell for 24 h. The infected cells were subjected to ZnO or TNF-α treatment, as indicated. Following treatment, luciferase activity was measured using the Luciferase Assay System (Promega, Madison, WI), according to the manufacturer's instructions.

2.9. Characterization of particle size distribution of ZnO

The particle size distribution of ZnO particles in the culture medium was analyzed using a Brookhaven *90Plus* Nanoparticle Size Analyzer (Brookhaven Instruments Corp., Long Island, USA) equipped with a 635-nm dio-laser of 35 mW. Based on the dynamic light scattering (DLS) technique, the *90Plus* is suitable for measuring particle size distributions from approximately 2 nm to approximately 3 μm in any liquid. To avoid the interference of absorption at 635 nm by phenol red and potential particles in FBS, after sonication for 30 s, ZnO suspensions (30 μg/ml) of each size (50 nm or 100 nm) were prepared in phenol red-free and FBS-free M199 medium. After incubation for 2, 6 or 24 h at RT, supernatants of each ZnO suspension were taken for particle diameter measurements.

2.10. Statistics

Each experiment was performed independently at least three times. The statistical analysis was expressed using the

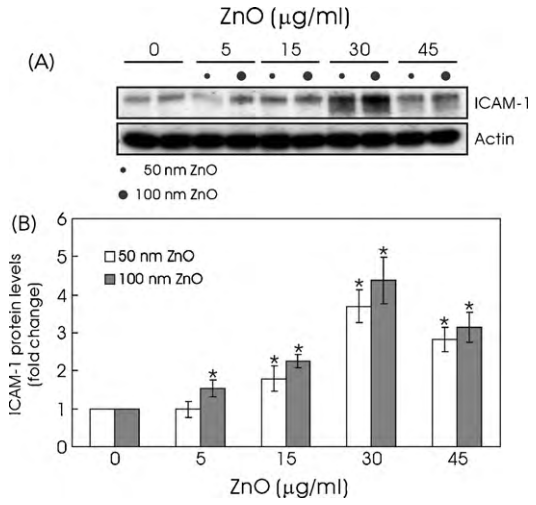

Fig. 2. ZnO induces ICAM-1 protein expression in a dose-dependent manner. HUVECs were left untreated or treated with 5, 15, 30 or 45 μg/ml of ZnO (50 nm or 100 nm) for 24 h. Following treatments, the cell lysates were analyzed for ICAM-1 and actin protein levels by immunoblot analysis. Representative immunoblot results were shown (A). The protein levels of ICAM-1 and actin were quantified (B). The data are presented as means ± SE ($n = 3$) and are expressed as relative ICAM-1 protein levels compared to that of the untreated control. $^*p < 0.05$ versus the untreated control.

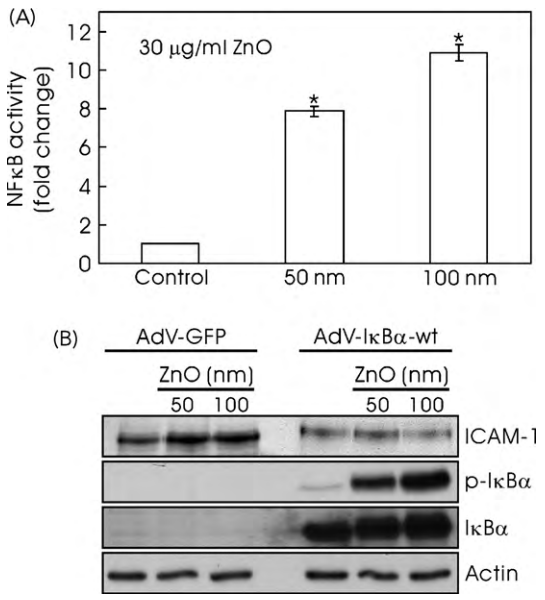

Fig. 3. ZnO induces ICAM-1 protein expression in an NF-κB-dependent manner. (A) To analyze NFκB reporter activity, HUVECs were infected with the recombinant adenovirus AdV-NFκB-Luc for 24 h. The infected cells were left untreated or treated with 30 μg/ml of ZnO (50 nm or 100 nm) for another 24 h. Following treatments, luciferase activity was determined. The data are presented as means ± SE ($n = 3$) and are expressed as relative NF-κB activity compared to that of the untreated control. $^*p < 0.05$ versus the untreated control. (B) To determine the role of IκBα, HUVECs were infected with a recombinant adenovirus (AdV-GFP or AdV-IκBα-wt) for 24 h. The infected cells were left untreated or treated with 30 μg/ml of ZnO (50 nm or 100 nm) for 24 h. Following treatments, the cell lysates were analyzed for protein levels of ICAM-1, IκBα phosphorylation (p-IκBα), IκBα, and actin by immunoblot analysis.

mean ± standard error (SE) from each independent experiment. To avoid statistical bias, a nonparametric test of Mann–Whiney *U* tests was used to determine statistical significance of the differences between experimental groups. Differences were considered statistically significant when $p < 0.05$. Analyses were carried out using the Statistical Package for Social Sciences (SPSS) version 12.0 (SPSS Inc., Chicago, IL, USA).

3. Results

3.1. Characterization of ZnO effects on HUVECs

The effects of ZnO on HUVECs were determined using a cytotoxicity assay, cell proliferation assay, and measurement of intracellular GSH levels. HUVECs were treated with 50-nm or 100-nm ZnO particles (ranging from 0.5 to 75 μg/ml) for 24 h and, as shown in Fig. 1A, in general, the ZnO treatments of two different particle sizes caused very similar cytotoxic patterns. A marked drop in survival rate was observed when the ZnO concentration was increased to 45 μg/ml. To evaluate the effect of ZnO on cell proliferation, treatment with lower concentrations of ZnO (0.1, 0.3, 1 or 3 μg/ml) for 5 days resulted in increases in cell proliferation by 22% ($p < 0.01$), 18% ($p < 0.05$), 14% ($p < 0.05$), and 3%, respectively, for 50-nm ZnO and by 20% ($p < 0.01$), 14% ($p < 0.01$), 10% ($p < 0.01$), and 6%, respectively, for 100-nm ZnO (Fig. 1B). Since there is a possible role for ZnO particles in the generation of oxidative stress, we further analyzed the intracellular glutathione status in response to ZnO treatment. As shown in Fig. 1C, both types of ZnO particles caused a similar dose-dependent increase in GSSG (oxidized form of glutathione). Treatment with ZnO concentrations of ≤45 μg/ml resulted in no marked change in total glutathione levels in HUVECs.

3.2. ZnO induces ICAM-1 protein expression in an NF-κB-dependent manner

Based on cytotoxicity results, ZnO treatments of ≤45 μg/ml were adopted to determine ICAM-1 protein expression, an indicator of the inflammatory response of vascular endothelium, using an immunoblot assay. As shown in Fig. 2, treatments with each type of ZnO particle in concentrations ranging from 5 to 30 μg/ml induced similar dose-dependent increases in ICAM-1 protein expression, When ZnO was increased to 45 μg/ml, however, the intensity of ICAM-1 protein induction was markedly attenuated, possibly due to ZnO-induced cytotoxicity.

To determine the role of NF-κB in the regulation of ZnO-induced ICAM-1 expression, we first analyzed the NF-κB reporter activity of HUVECs in response to 30 μg/ml of ZnO treatment. As shown in Fig. 3A, 50 and 100-nm ZnO treatments caused 7.9-fold ($p < 0.05$) and 10.9-fold ($p < 0.05$) increases, respectively, in the NF-κB reporter activity of HUVECs. Then, using an adenovirus-mediated expression system, we investigated whether the ZnO treatment was able to induce IκBα phosphorylation and whether overexpression of IκBα could block ZnO-induced ICAM-1 expression. As shown in Fig. 3B, in the adenovirus-infection control experiments (AdV-GFP), both 50 and 100-nm ZnO particles caused increases in ICAM-1 expression, but there was no detectable IκBα phosphorylation, and IκBα degradation was barely observed. This phenomenon was most likely due to the rapid polyubiquitination and subsequent degradation of phosphorylated IκBα by the 26S proteasome [26]. Meanwhile, in adenovirus-mediated overexpression of IκBα experiments (AdV-IκBα-wt), ZnO-induced ICAM-1 expression was totally inhibited, accompanied by pronounced IκBα expression and ZnO-induced IκBα phosphorylation. Because of the abundant IκBα expression by adenovirus system, we will be able to detect the IκBα phosphorylation.

3.3. TNF-α induces ICAM-1 protein expression in an NF-κB-dependent manner

We employed TNF-α, a typical inflammatory cytokine, to evaluate the relative potency of ZnO in the activation of the inflammatory response of vascular endothelium. As shown in Fig. 4A, treatment of

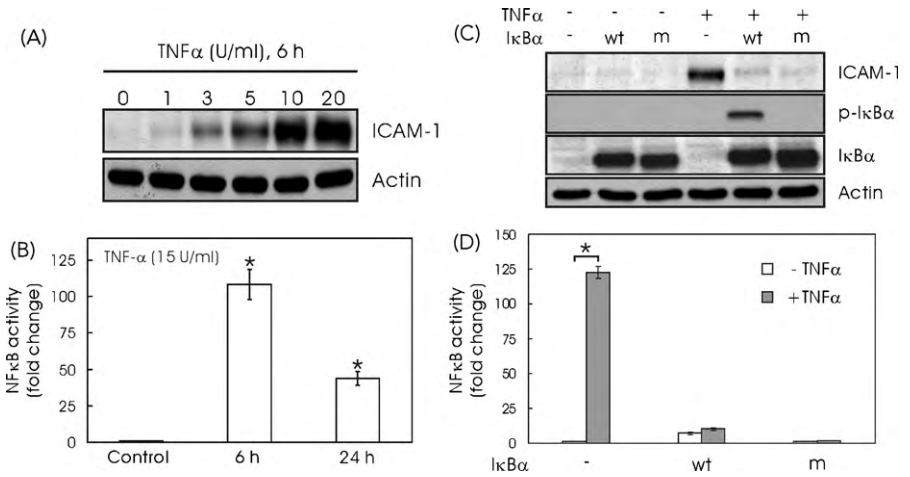

Fig. 4. TNF-α induces ICAM-1 protein expression in an NF-κB-dependent manner. (A) HUVECs were left untreated or treated with TNF-α (1, 3, 5, 10 or 20 U/ml) for 6 h. (B) HUVECs were infected with the recombinant adenovirus AdV-NFκB-Luc for 24 h. The infected cells were left untreated or treated with TNF-α (15 U/ml) for 6 and 24 h. (C) HUVECs were infected with AdV-GFP (−), AdV-IκBα-wt (wt) or AdV-IκBα-m (m) recombinant adenovirus for 24 h. The infected cells were left untreated (−) or treated (+) with TNF-α (15 U/ml) for 6 h. (D) HUVECs were co-infected with AdV-NFκB-Luc and one of the recombinant adenoviruses [AdV-GFP (−), AdV-IκBα-wt (wt) or AdV-IκBα-m (m)]. The infected cells were left untreated or treated with TNF-α (15 U/ml) for 6 h. For immunoblot analysis (A and C), the cell lysates were analyzed for protein levels of ICAM-1, IκBα phosphorylation (p-IκBα), IκBα, and actin. For luciferase activity measurement (B and D), the data are presented as means ± SE ($n = 3$) and are expressed as relative NF-κB activity compared to that of the untreated control. *$p < 0.05$ versus the untreated control.

HUVECs with TNF-α (1, 3, 5, 10 or 20 U/ml) for 6 h resulted in dose-dependent increases in ICAM-1 protein expression. Treatment with 15 U/ml TNF-α for 6 h or 24 h caused 108-fold ($p < 0.05$) and 44-fold ($p < 0.05$) increases, respectively, in NF-κB reporter activity (Fig. 4B). Adenovirus-mediated overexpression of either wild-type or mutant IκBα almost completely blocked TNF-α-induced ICAM-1 protein expression; no IκBα phosphorylation was detected in samples in which the IκBα mutant was overexpressed (Fig. 4C). Similarly, adenovirus-mediated overexpression of wild-type or mutant IκBα significantly blocked TNF-α-induced NF-κB reporter activation (Fig. 4D). Therefore, the results from the ICAM-1 expression and NF-κB reporter activity assays indicated that ZnO-induced responses were relatively much weaker than those induced by TNF-α.

3.4. ZnO synergistically enhances TNF-α-induced ICAM-1 expression

To determine the combined effects of ZnO and TNF-α on ICAM-1 expression, we treated HUVECs with different concentrations of TNF-α (0.15 U/ml, 1.5 U/ml or 15 U/ml) in the presence of ZnO (30 μg/ml) and then analyzed ICAM-1 protein expression in the cells. As shown in Fig. 5, TNF-α (0.15 U/ml, 1.5 U/ml or 15 U/ml) alone caused a 1.1-, 3.5- or 7.0-fold induction, respectively, of ICAM-1 expression. In the presence of 50-nm ZnO, ICAM-1 induction was further enhanced to 5.5-, 11.6- or 18.4-fold, respectively. In the presence of 100-nm ZnO, ICAM-1 induction was further enhanced to 5.2-, 12.1- or 19.2-fold, respectively. On the basis of these data, we found that ZnO was able to synergistically enhance TNF-α-induced ICAM-1 expression in HUVECs.

3.5. Both ZnO particle sizes agglomerated to similar sizes in culture medium.

Here, we demonstrated that ZnO particles induce inflammatory responses in vascular endothelial cells via NF-κB signaling. However, our results failed to differentiate the biological effects induced by 50-nm vs. 100-nm ZnO particles. Time-course changes in particle size distributions of the two types of ZnO particles in cell culture medium were characterized (Supplementary data). For 50-nm ZnO particles, the intensity peaks were initially centered at diameters of 390 and 2240 nm (0 h) and then gradually shifted down to smaller diameters (2 and 6 h). After incubation for 24 h, the major intensity peak was centered at a diameter of 270 nm. For 100-nm ZnO particles, the intensity peak was initially centered at diameters of 460 nm (0 h) and then gradually shifted down to smaller diameters (2 and 6 h). After incubation for 24 h, the major intensity peaks were distributed between diameters of 180 and 300 nm. These data indicate that both types of ZnO particles readily agglomerate in culture medium, as the agglomerated ZnO particles tended to precipitate gradually, and the particle sizes of the two ZnO particle types that remained in suspension became very similar after a 24 h-incubation in culture medium.

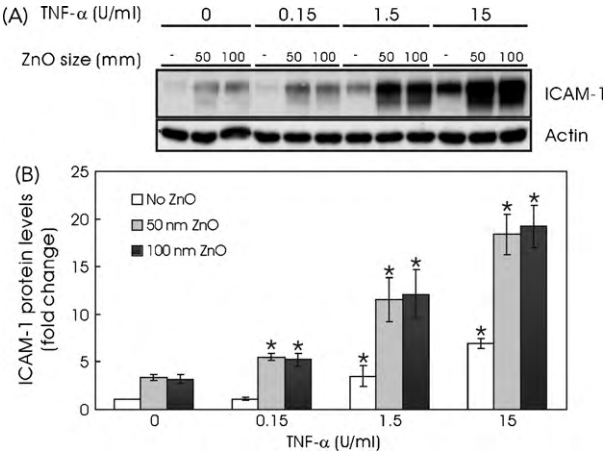

Fig. 5. ZnO synergistically enhances TNF-α-induced ICAM-1 expression. HUVECs cells were left untreated or treated with 30 μg/ml of ZnO (50 nm or 100 nm) for 24 h. Then, the cells were treated with TNF-α (0.15, 1.5 or 15 U/ml) for another 6 h. Following treatments, the cell lysates were analyzed for protein levels of ICAM-1 and actin by immunoblot analysis. Representative immunoblot results were shown (A). The protein levels of ICAM-1 and actin were quantified (B). The data are presented as means ± SE ($n = 3$) and are expressed as relative ICAM-1 protein levels compared to that of the untreated control. *$p < 0.05$ versus the TNF-α untreated control of each set (No ZnO, 50 nm ZnO, or 100 nm ZnO).

4. Discussion

One of the initial events in atherogenesis is the activation of vascular endothelial cells, which then express adhesion molecules such as vascular adhesion molecule-1 (VCAM-1), endothelial leukocyte adhesion molecule (E-selectin), and ICAM-1 [27]. Proinflammatory stimuli, including TNF-α, increase adhesion molecule expression and contribute to the initial phase of atherogenesis [9]. ICAM-1, continuously present in low concentrations in the membranes of leukocytes and endothelial cells, is a ligand for LFA-1 (integrin), a receptor found on leukocytes [28]. Cytokines or other proinflammatory mediators induce adhesion molecule expression and facilitate leukocyte attachment to vascular endothelial surfaces via ICAM-1/LFA-1 [29,30]. The adhesion of monocytes to the arterial wall and their subsequent infiltration and differentiation into macrophages is a crucial step in the development of atherosclerosis [31].

In the present study, the MTT cytotoxicity assay was used to define the toxic effects of ZnO particles on HUVECs (Fig. 1A). Increased cell proliferation by low levels of ZnO treatment ($\leq$3 μg/ml) (Fig. 1B) and slightly increased oxidative stress, as determined by GSSG formation, by 5 μg/ml ZnO treatment (Fig. 1C) support the hypothesis that low levels of oxidative stress may act as a second messenger in the regulation of cell proliferation [32]. Moreover, ZnO treatments resulted in increases in oxidative stress in a dose-dependent manner, leading to a marked drop in survival rate when the ZnO concentration was increased to 45 μg/ml. However, the cytotoxicity induced by 45 μg/ml ZnO, as shown by the MTT assay, seemed to be overestimated, as shown by microscopic observation. Indeed, a recent study reported that classical dye-based assays such as MTT and neutral red that determine cell viability produce biased results with some nanomaterials due to nanomaterial/dye interactions and/or nanomaterial adsorption of the dye or dye products [33]. In addition, MTT assay is based on the cleavage of MTT, a yellow tetrazolium salt, to purple formazan crystals by the succinate-tetrazolium reductase system, belonging to the respiratory chain of mitochondria. Therefore, the amount of formazan dye formed directly correlates to the number of metabolically active cells in culture [21].

Our previous study showed that arsenite alone was not able to induce adhesion molecule expression; instead, it enhances TNF-α-induced adhesion molecule expression in HUVECs through the regulation of redox-sensitive transcription factors, including NF-κB, in a GSH-sensitive manner [20]. In the present study, we demonstrated that ZnO treatments also caused increases in oxidative stress, as determined by GSSG formation, and activation of the redox-sensitive transcription factor NF-κB (Fig. 3A). These results suggested that ZnO and arsenite might play a similar role in modulation of adhesion molecule expression in vascular endothelial cells in response to proinflammatory cytokines, such as TNF-α. Indeed, we showed that ZnO did enhance TNF-α-induced ICAM-1 expression in HUVECs (Fig. 5). Moreover, it should be noted that ZnO alone induced ICAM-1 expression in HUVECs. Treatment of HUVECs with 30 μg/ml ZnO for 24 h resulted in the highest level of ICAM-1 expression (Fig. 2), with 8-fold and 11-fold increases in NF-κB reporter activity following 50 and 100-nm ZnO treatments, respectively (Fig. 3A). The critical role of NF-κB in ICAM-1 expression has been well established. However, it was very difficult to detect phosphorylation of IκBα in these protein lysates by immunoblot analysis, a phenomenon that is most likely due to the rapid polyubiquitination and subsequent degradation of phosphorylated IκBα by the 26S proteasome [26].

To further understand the role of NF-κB (or IκBα phosphorylation) in the regulation of ZnO-induced ICAM-1 expression, we constructed three recombinant adenoviruses, AdV-IκBα-wt (expressing wild-type IκBα under the CMV promoter with a built-in GFP tracer), AdV-IκBα-m (expressing mutated IκBα under the CMV promoter with a built-in GFP tracer), and AdV-GFP (expressing a built-in GFP tracer). Our results clearly showed that overexpression of IκBα (either wild-type or mutated) by recombinant adenoviruses markedly abolished ZnO- or TNF-α-induced ICAM-1 expression (Figs. 3B and 4C) as well as TNF-α-induced NF-κB reporter activation (Fig. 4D). Moreover, using this overexpression system, ZnO- or TNF-α-induced IκBα phosphorylation at residue 32 was much easier to detect (Figs. 3B and 4C). Meanwhile, AdV-IκBα-m contains a mutated form of IκBα with serine-to-alanine mutations at residues 32 and 36, and therefore, as expected, IκBα phosphorylation in samples from those AdV-IκBα-m-infected cells was not detected (Fig. 4C).

Although the present study clearly demonstrated that ZnO could activate inflammatory ICAM-1 expression in HUVECs, it was important to further investigate the potency of the ZnO-inflammatory response compared to the response induced by the typical inflammation cytokine TNF-α. Treatment with ZnO (30 μg/ml) for 24 h resulted in a 3- to 4-fold increase in ICAM-1 expression (Figs. 2 and 5), while treatment with TNF-α (15 U/ml) for 6 h resulted in a 7-fold increase in ICAM-1 expression (Fig. 5). Our data suggest that the levels of ICAM-1 expression induced by 30 μg/ml ZnO were approximately the same as those induced by 1.5 U/ml TNF-α (Fig. 5). Moreover, treatment with 50 and 100-nm ZnO (30 μg/ml, 24 h) caused 7.9- and 10.9-fold increases, respectively, in NF-κB reporter activation (Fig. 3), while treatment with TNF-α (15 U/ml) for 6 h and 24 h resulted in 108- indicate that the levels of NF-κB reporter activity induced by 15 U/ml TNF-α were much and 44-fold increases, respectively, in NF-κB reporter activity (Fig. 4). Our present results higher than those induced by 30 μg/ml ZnO.

The present study revealed that ZnO synergistically enhanced TNF-α-induced ICAM-1 expression in HUVECs. In general, ZnO further enhanced TNF-α-induced ICAM-1 expression by 3- to 5-fold, depending on the TNF-α dosage. This finding suggests that in the presence of an inflammatory cytokine such as TNF-α, ZnO-induced inflammatory responses could be much higher than originally expected. Our previous study showed that arsenite enhanced TNF-α-induced adhesion molecule expression in vascular endothelial cells through the regulation of redox-sensitive transcription factors, including NF-κB [20]. Both ZnO and arsenite can enhance TNF-α-induced adhesion molecule expression in vascular endothelial cells. However, there are three major differences among the effects induced by these two chemicals. First, ZnO alone but not arsenite alone is able to induce adhesion molecule expression. Second, ZnO causes increases in GSSG with no effect on total glutathione, whereas arsenite causes increases in both GSSG and total glutathione. Third, the enhanced TNF-α-induced adhesion molecule expression induced by ZnO is higher than that induced by arsenite.

The usefulness of *in vitro* systems to allow nanoparticles to be incorporated into cultured cells has been clearly demonstrated by several studies [33–35]. However, the present study failed to differentiate the biological effects induced by 50 and 100-nm ZnO particles, possibly due to the agglomeration of ZnO particles in culture medium. A recent study employed dynamic light scattering and transmission electron microscopy to determine the effects of sonication, temperature, and exposure time on nanoparticle size in culture medium. All particles were much larger than their predosed size, suggesting significant agglomeration [33]. Moreover, it was shown that nanoparticles tightly interacted with proteins in the culture medium to promote agglomeration [36]. Thus, without using any nanoparticle dispersion technique, nanoparticles could possibly be incorporated into culture cells, but this incorporation would be accompanied by the unavoidable agglomeration of nanoparticles in the culture medium.

5. Conclusions

Using HUVECs as an *in vitro* system, this study reveals several important new findings. First, ZnO particles alone can induce inflammatory ICAM-1 expression. Second, like TNF-α, ZnO particles induce ICAM-I expression via NF-κB signaling. Third, ZnO particles synergistically enhance TNF-α-induced ICAM-1 expression.

Acknowledgements

This work was supported by grants from the National Science Council [NSC96-2314-B-400-004, NSC97-2314-B-400-003-MY3], the National Health Research Institutes (EO-097-PP-07, EO-098-PP-05), and the Institute of Occupational Safety & Health (IOSH98-M323) in Taiwan.

Appendix A. Supplementary data

Supplementary data associated with this article can be found, in the online version, at doi:10.1016/j.jhazmat.2010.07.010.

References

[1] A.D. Maynard, R.J. Aitken, T. Butz, V. Colvin, K. Donaldson, G. Oberdorster, M.A. Philbert, J. Ryan, A. Seaton, V. Stone, S.S. Tinkle, L. Tran, N.J. Walker, D.B. Warheit, Safe handling of nanotechnology, Nature 444 (2006) 267–269.
[2] J.M. Samet, F. Dominici, F.C. Curriero, I. Coursac, S.L. Zeger, Fine particulate air pollution and mortality in 20 U.S. cities, 1987–1994, N. Engl. J. Med. 343 (2000) 1742–1749.
[3] A. Peters, D.W. Dockery, J.E. Muller, M.A. Mittleman, Increased particulate air pollution and the triggering of myocardial infarction, Circulation 103 (2001) 2810–2815.
[4] C.A. Pope, R.T. 3rd, G.D. Burnett, M.J. Thurston, E.E. Thun, D. Calle, J.J. Krewski, Godleski, Cardiovascular mortality and long-term exposure to particulate air pollution: epidemiological evidence of general pathophysiological pathways of disease, Circulation 109 (2004) 71–77.
[5] W.G. Kreyling, M. Semmler, F. Erbe, P. Mayer, S. Takenaka, H. Schulz, G. Oberdorster, A. Ziesenis, Translocation of ultrafine insoluble iridium particles from lung epithelium to extrapulmonary organs is size dependent but very low, J. Toxicol. Environ. Health A 65 (2002) 1513–1530.
[6] A. Nemmar, P.H. Hoet, D. Dinsdale, J. Vermylen, M.F. Hoylaerts, B. Nemery, Diesel exhaust particles in lung acutely enhance experimental peripheral thrombosis, Circulation 107 (2003) 1202–1208.
[7] A. Nemmar, P.H. Hoet, B. Vanquickenborne, D. Dinsdale, M. Thomeer, M.F. Hoylaerts, H. Vanbilloen, L. Mortelmans, B. Nemery, Passage of inhaled particles into the blood circulation in humans, Circulation 105 (2002) 411–414.
[8] A. Gojova, B. Guo, R.S. Kota, J.C. Rutledge, I.M. Kennedy, A.I. Barakat, Induction of inflammation in vascular endothelial cells by metal oxide nanoparticles: effect of particle composition, Environ. Health Perspect. 115 (2007) 403–409.
[9] R. Ross, Atherosclerosis—an inflammatory disease, N. Engl. J. Med. 340 (1999) 115–126.
[10] N. Sattar, Inflammation and endothelial dysfunction: intimate companions in the pathogenesis of vascular disease? Clin. Sci. (Lond.) 106 (2004) 443–445.
[11] J.A. Berliner, D.S. Schwartz, M.C. Territo, A. Andalibi, L. Almada, A.J. Lusis, D. Quismorio, Z.P. Fang, A.M. Fogelman, Induction of chemotactic cytokines by minimally oxidized LDL, Adv. Exp. Med. Biol. 351 (1993) 13–18.
[12] J. Hulthe, B. Fagerberg, Circulating oxidized LDL is associated with subclinical atherosclerosis development and inflammatory cytokines (AIR Study), Arterioscler. Thromb. Vasc. Biol. 22 (2002) 1162–1167.
[13] Y. Xu, M. Rojkind, M.J. Czaja, Regulation of monocyte chemoattractant protein 1 by cytokines and oxygen free radicals in rat hepatic fat-storing cells, Gastroenterology 110 (1996) 1870–1877.
[14] A.V. Sterpetti, A. Cucina, A.R. Morena, S. Di Donna, L.S. D'Angelo, A. Cavalarro, S. Stipa, Shear stress increases the release of interleukin-1 and interleukin-6 by aortic endothelial cells, Surgery 114 (1993) 911–914.
[15] K. Sakai, M. Mohtai, J. Shida, K. Harimaya, S. Benvenuti, M.L. Brandi, T. Kukita, Y. Iwamoto, Fluid shear stress increases interleukin-11 expression in human osteoblast-like cells: its role in osteoclast induction, J. Bone Miner. Res. 14 (1999) 2089–2098.
[16] M. Humbert, G. Monti, F. Brenot, O. Sitbon, A. Portier, L. Grangeot-Keros, P. Duroux, P. Galanaud, G. Simonneau, D. Emilie, Increased interleukin-1 and interleukin-6 serum concentrations in severe primary pulmonary hypertension, Am. J. Respir. Crit. Care Med. 151 (1995) 1628–1631.
[17] J.L. Young, P. Libby, U. Schonbeck, Cytokines in the pathogenesis of atherosclerosis, Thromb. Haemost. 88 (2002) 554–567.
[18] A.J. Lusis, Atherosclerosis, Nature 407 (2000) 233–241.
[19] M.A. Gimbrone Jr., R.S. Cotran, J. Folkman, Human vascular endothelial cells in culture. Growth and DNA synthesis, J. Cell Biol. 60 (1974) 673–684.
[20] T.C. Tsou, S.C. Yeh, E.M. Tsai, F.Y. Tsai, H.R. Chao, L.W. Chang, Arsenite enhances tumor necrosis factor-alpha-induced expression of vascular cell adhesion molecule-1, Toxicol. Appl. Pharmacol. 209 (2005) 10–18.
[21] T. Mosmann, Rapid colorimetric assay for cellular growth and survival: application to proliferation and cytotoxicity assays, J. Immunol. Methods 65 (1983) 55–63.
[22] T.C. Tsou, S.C. Yeh, F.Y. Tsai, L.W. Chang, The protective role of intracellular GSH status in the arsenite-induced vascular endothelial dysfunction, Chem. Res. Toxicol. 17 (2004) 208–217.
[23] J.B. Huppa, H.L. Ploegh, The eS-Sence of -SH in the ER, Cell 92 (1998) 145–148.
[24] A.M. Gomez-Foix, W.S. Coats, S. Baque, T. Alam, R.D. Gerard, C.B. Newgard, Adenovirus-mediated transfer of the muscle glycogen phosphorylase gene into hepatocytes confers altered regulation of glycogen metabolism, J. Biol. Chem. 267 (1992) 25129–25134.
[25] W.J. McGrory, D.S. Bautista, F.L. Graham, A simple technique for the rescue of early region I mutations into infectious human adenovirus type 5, Virology 163 (1988) 614–617.
[26] D. Krappmann, C. Scheidereit, A pervasive role of ubiquitin conjugation in activation and termination of IkappaB kinase pathways, EMBO Rep. 6 (2005) 321–326.
[27] M.I. Cybulsky, M.A. Gimbrone Jr., Endothelial expression of a mononuclear leukocyte adhesion molecule during atherogenesis, Science 251 (1991) 788–791.
[28] R. Rothlein, M.L. Dustin, S.D. Marlin, T.A. Springer, A human intercellular adhesion molecule (ICAM-1) distinct from LFA-1, J. Immunol. 137 (1986) 1270–1274.
[29] T. Collins, Endothelial nuclear factor-kappa B and the initiation of the atherosclerotic lesion, Lab. Invest. 68 (1993) 499–508.
[30] L. Yang, R.M. Froio, T.E. Sciuto, A.M. Dvorak, R. Alon, F.W. Luscinskas, ICAM-1 regulates neutrophil adhesion and transcellular migration of TNF-alpha-activated vascular endothelium under flow, Blood 106 (2005) 584–592.
[31] C.K. Glass, J.L. Witztum, Atherosclerosis. The road ahead, Cell 104 (2001) 503–516.
[32] M. Karin, E. Shaulian, AP-1: linking hydrogen peroxide and oxidative stress to the control of cell proliferation and death, IUBMB Life 52 (2001) 17–24.
[33] N.A. Monteiro-Riviere, A.O. Inman, L.W. Zhang, Limitations and relative utility of screening assays to assess engineered nanoparticle toxicity in a human cell line, Toxicol. Appl. Pharmacol. 234 (2009) 222–235.
[34] J.G. Rouse, J. Yang, A.R. Barron, N.A. Monteiro-Riviere, Fullerene-based amino acid nanoparticle interactions with human epidermal keratinocytes, Toxicol. In Vitro 20 (2006) 1313–1320.
[35] J.P. Ryman-Rasmussen, J.E. Riviere, N.A. Monteiro-Riviere, Surface coatings determine cytotoxicity and irritation potential of quantum dot nanoparticles in epidermal keratinocytes, J. Invest. Dermatol. 127 (2007) 143–153.
[36] R.C. Murdock, L. Braydich-Stolle, A.M. Schrand, J.J. Schlager, S.M. Hussain, Characterization of nanomaterial dispersion in solution prior to in vitro exposure using dynamic light scattering technique, Toxicol. Sci. 101 (2008) 239–253.